

Voltammetric Determination of Sudan I by Using Bi₂WO₆ Nanosheets Modified Glassy Carbon Electrode

Venkatachalam Vinothkumar¹, Arumugam Sangili¹, Shen-Ming Chen^{1,*},
Tse-Wei Chen^{1,2}, Manickavasagan Abinaya¹, Venkatachalam Sethupathi¹

¹ Department of Chemical Engineering and Biotechnology, National Taipei University of Technology, No. 1, Chung-Hsiao East Road, Section 3, Taipei 10608, Taiwan, ROC.

² Research and Development Center for Smart Textile Technology, National Taipei University of Technology, No.1, Section 3, Chung-Hsiao East Road, Taipei 106, Taiwan.

*E-mail: smchen1957@gmail.com

Received: 3 November 2019 / Accepted: 19 December 2019 / Published: 10 February 2020

The as-synthesized nanomaterials have been completely characterized by X-ray powder spectroscopy, frontier infrared spectroscopy, Raman spectroscopy, scanning electron spectroscopy, energy dispersive spectroscopy, and mapping analysis as well as electrochemical measurements. The structural and morphological characterizations show the sheet-like structure of bismuth-doped tungsten oxide. The as-synthesized Bi₂WO₆ nanosheets were utilized for the electrochemical determination of Sudan I. The results confirm that the bismuth-doped material has enhanced electrocatalytic activities compared to the undoped tungsten oxides. Furthermore, the reaction kinetics of the electrochemical oxidation of Sudan I using the Bi₂WO₆ modified electrode surface was a diffusion-controlled process, and which involves two-proton and two-electron transfer mechanisms. The analytical measurements were employed by DPV techniques under optimal conditions, and thus shows a wide linearity range of 0.02 to 114.6 μM with high sensitivity and low detection limit of 3.0563 μA μM⁻¹ and 0.002 μM (S/N = 3), respectively. Besides, the Bi₂WO₆ modified electrodes demonstrate superior electrochemical performances towards the detection of Sudan I than the previously reported articles. Finally, the as-fabricated sensor has been applied to the real-time application for sensitive determination of Sudan I in food samples, such as apple juice and chili powder with acceptable recoveries.

Keywords: Bi₂WO₆, Sudan I, food coloring agent, electrochemical sensor.

1. INTRODUCTION

Sudan I (1-phenylazo-2-naphthol) is a synthetic azo dye and commonly used as a coloring material in industrial products, including textiles, shoes, plastics, oils, floor polishes, printing inks, and cosmetics [1]. Specifically, Sudan I, are also found as food additive materials including chili powder, sauces,

chutneys and readymade meals due to its bright and rich red color, low cost, and colorfastness. The carcinogenic properties of Sudan I have been found in the 1970s and were no longer permitted by any national and international food regulation act. Although the European Union has banned the use of Sudan I compounds as food dyes [2,3]. Nevertheless, Sudan I is still utilized as an additive in foodstuffs to improve the visual attractiveness [4]. Thus, it is essential to fabricate a reliable, rapid, high-selective, and sensitive electrochemical sensor for the detection of Sudan I. For the electrochemical determination of Sudan I, a various methods have been reported previously, such as gas chromatography, mass spectroscopy detection [5], HPLC [6], HPLC/APCI-MS [7], SERS [8], capillary liquid chromatography [9], and electrochemical detection [10]. However, these methods usually complex and needs pre-treatment process, and expansive equipment, thus make high time consumption and cost. The electrochemical methods have attracted wide attention because of their fastness, convenience, high sensitivity, and selectivity.

Among them, bismuth-containing semiconductors exhibit a great potential application in degradation of organic pollutants, water purification, Li-ion battery, and sensors, due to their nontoxicity, good stability, extraordinary band structure, electrical conductivity, and lower valance band levels. The several bismuth modified semiconducting materials utilized for the above-mentioned applications are as follows BiVO_4 [11], Bi_2MoO_6 [12], $\text{Bi}_2\text{O}_2\text{CO}_3$ [13], $\text{Bi}_4\text{Ti}_3\text{O}_{12}$ [14], Bi_2WO_6 [15]. Bismuth tungstate (Bi_2WO_6) is one of the simplest materials from the Aurivillius oxide families of layered perovskites. It has a variety of fascinating physical and chemical properties and broad potential utilities for the catalysts, microwave optical fibers, ferroelectric pyro electrical devices, piezoelectrical, and sensor devices [16-20]. Owing to its tremendous semiconducting properties, it has been widely used in the field of photocatalysis, solar cells, capacitors, and electrochemical sensing applications [21-23].

In this work, we report, the preparation of bismuth tungstate (Bi_2WO_6) nanosheets using a simple co-precipitation method and applied to the sensitive detection of Sudan I for the first time. It is found that the Bi_2WO_6 modified glassy carbon electrode (GCE) exhibits good electrochemical activity towards the sensing of Sudan I. Also, the as-fabricated Bi_2WO_6 /GCE sensor displayed a superior sensitivity, wide linear range, very lower detection limit, and a good recovery in real samples analysis.

2. EXPERIMENTAL

2.1. Chemical and materials

Sudan I, $\text{Na}_2\text{WO}_4 \cdot 2\text{H}_2\text{O}$, $\text{Bi}(\text{NO}_3)_3 \cdot 5\text{H}_2\text{O}$ were purchased from Sigma Aldrich. All other reagents were of analytical grades and purchased from Sigma Aldrich. The Na_2HPO_4 and NaH_2PO_4 were used for the preparation of buffer solution (PBS). All experiments were conducted using Millipore water (MW) (18.25 M W/cm, Milli-Q).

2.2. Preparation of Bi_2WO_6 nanosheets

The Bi_2WO_6 nanosheets were synthesized by the co-precipitation method. In a typical synthesis procedure, the stoichiometric ratio of $\text{Bi}(\text{NO}_3)_3 \cdot 5\text{H}_2\text{O}$ and $\text{Na}_2\text{WO}_4 \cdot 2\text{H}_2\text{O}$ precursors were added into 100 mL Millipore water and followed by magnetic stirring for 30 min. Then the addition of 10 mL of 0.5 M NaOH solution was added to the above mixture. The obtained precipitate was washed by water/ethanol several times and allowed to dry at 80 °C for 12 h. Further, the product was calcined for 2 h at 350 °C. The obtained Bi_2WO_6 nanosheets were denoted as BWO NSs.

2.3. Characterization

The structure and morphology were characterized by field-emission scanning electron microscope (FE-SEM, JEOL-JSM 7610F). The powder X-ray diffraction (PXRD) studies were performed on an (XRD, X'pert3 range Malvern Panalytical, United Kingdom) with Cu $K\alpha$ radiation ($k = 1.54 \text{ \AA}$). Fourier transform infrared (FT-IR) spectra of the synthesized material was characterized by using a JASCO FT-IR 4600LE spectrometer between 4000 cm^{-1} and 400 cm^{-1} applying KBr pellets. Through scanning electron microscope (SEM) using the Quanta 250FEG instrument, the elemental composition and morphology of all samples are examined. All electrochemical measurements were using the standard three-electrode system were carried out on a CHI 660 and CHI 1205B electrochemical instruments (CH instruments) with GCE as the working electrode, a platinum wire (Pt wire) as the counter electrode, and an Ag/AgCl (saturated KCl) as the reference electrode. The electrochemical performances of the modified GCE for the determination of SI were assessed by electrochemical impedance spectroscopy (EIS), cyclic voltammetry (CV) and difference pulse voltammetry (DPV) techniques.

2.4. Fabrication of Bi_2WO_6 -modified electrodes

Firstly, the GCE was polished by polishing cloth using alumina slurry (0.05 μm) and washed with MW and ethanol until a mirror-like surface was produced. The Bi_2WO_6 -modified electrodes were prepared by first dispersing 5 mg mL^{-1} of the as-prepared Bi_2WO_6 material in water, then sonication for 45 min. subsequently, 6.0 μL suspension was drop cast on the surface of pre-cleaned GCE and drying in an oven at 50 °C. The fabricated electrode was stored at 4 °C, when not in use.

2.5. Sample preparation

Apple juice and chili powder samples were treated as the following method. 10.0 ml of apple juice and 10.0 g of chili powder was weighed and mixed with 30 mL ethanol. The mixture was ultrasonication for 30 min and the solution was filtered. The treatment was repeated three times, and filtered samples were diluted to volume with ethanol [24].

3. RESULTS AND DISCUSSION

3.1 Characterization of Bi_2WO_6 sample

The XRD patterns of the as-synthesized Bi_2WO_6 sample was shown in Fig. 1a. The different characteristic peak at $2\theta = 19.2, 21.5, 23.0, 28.2, 32.2, 32.6, 39.1, 42.6, 47.1, 55.5, 58.9, 63.6,$ and 66.7° , which could be indexed to the (012), (004), (111), (113), (200), (020), (024), (214), (220), (119), (1110), (129), and (228) plane of the orthorhombic phase of Bi_2WO_6 , respectively (JCPDS No. 73-1126) [25]. In Fig. 1b. showed the Raman spectra of Bi_2WO_6 exhibits a characteristic peak at 720 cm^{-1} that exhibits a splitted pattern due to the W-O distortion. A band at 637 cm^{-1} due to the $[\text{Bi}_2\text{O}_2]^{2+}$ stretching mode. The bands in the $100\text{-}450\text{ cm}^{-1}$ region can be attributed to the bending vibration of WO_6 octahedron, bending, and stretching vibration of BiO_6 polyhedron [26]. FT-IR spectra of Bi_2WO_6 is shown in Fig. 1c. The broad adsorption bands at $400\text{-}800\text{ cm}^{-1}$, which are assigned to Bi-O, stretching W-O, and bridging stretching modes W-O-W [27]. The broad adsorption band at 3440 cm^{-1} was assigned to -OH band. The results indicated that the formation of Bi_2WO_6 materials.

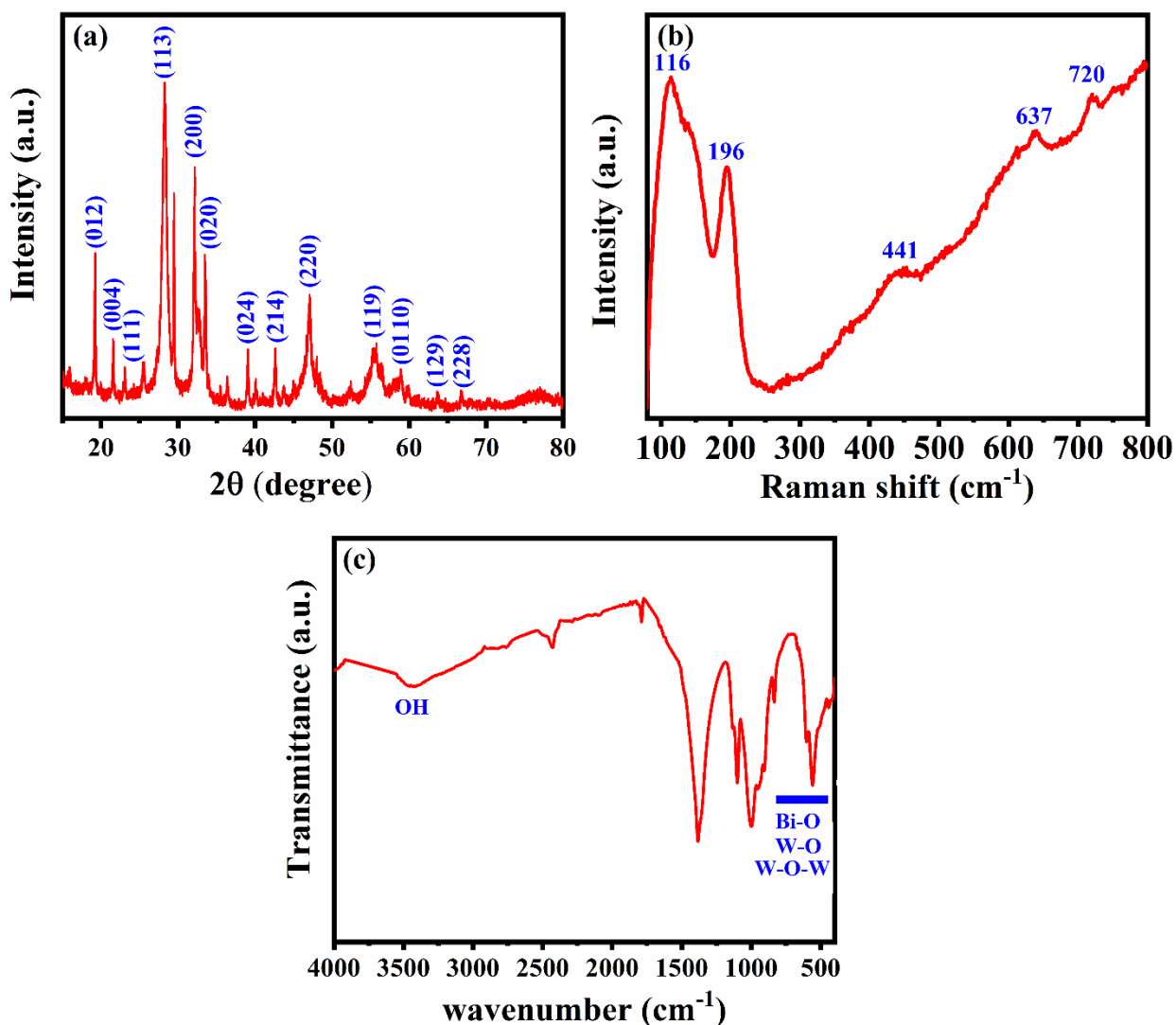


Figure 1. (a) XRD pattern and (b) Raman spectra and (c) FT-IR spectra of Bi_2WO_6 samples.

The FE-SEM images of as-prepared Bi_2WO_6 material without (Fig. 2a, b) and with (Fig. 2c, d) calcination temperature (50 °C and 350 °C), respectively. The surface morphology of Bi_2WO_6 before the calcination process shows the agglomerated particles.

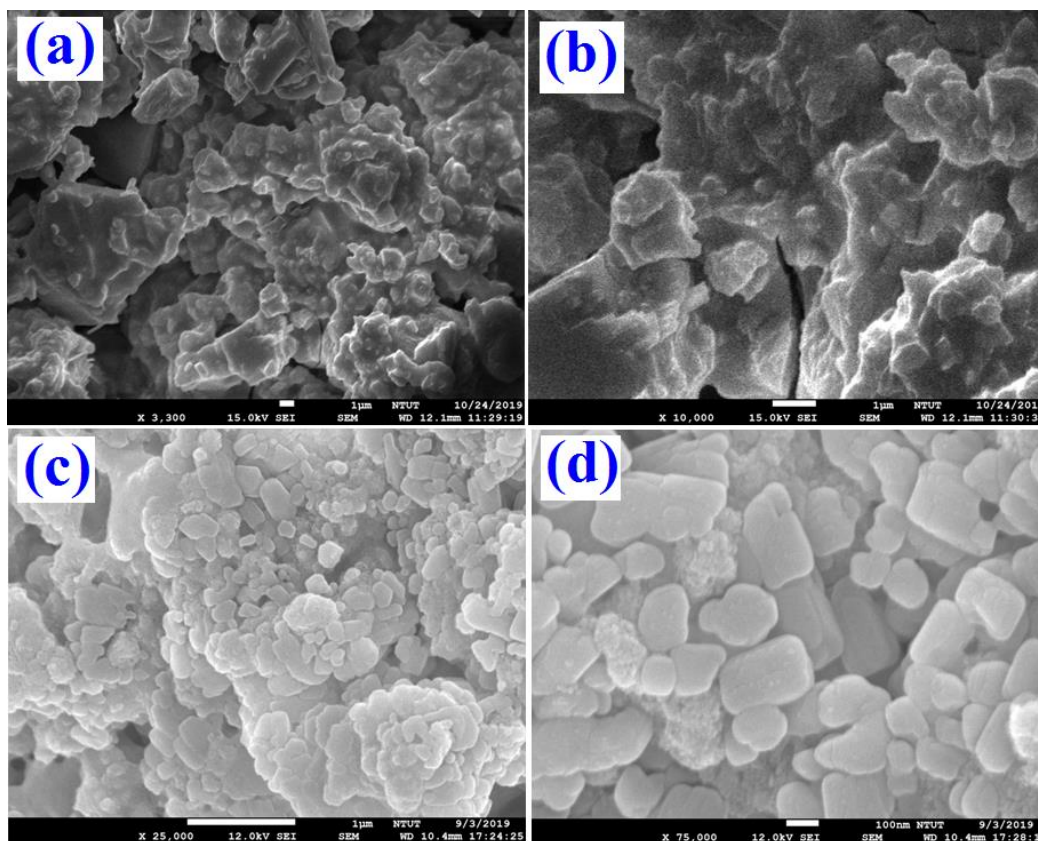


Figure 2. FE-SEM of (a, b) before and (c, d) after calcination of Bi_2WO_6 composites.

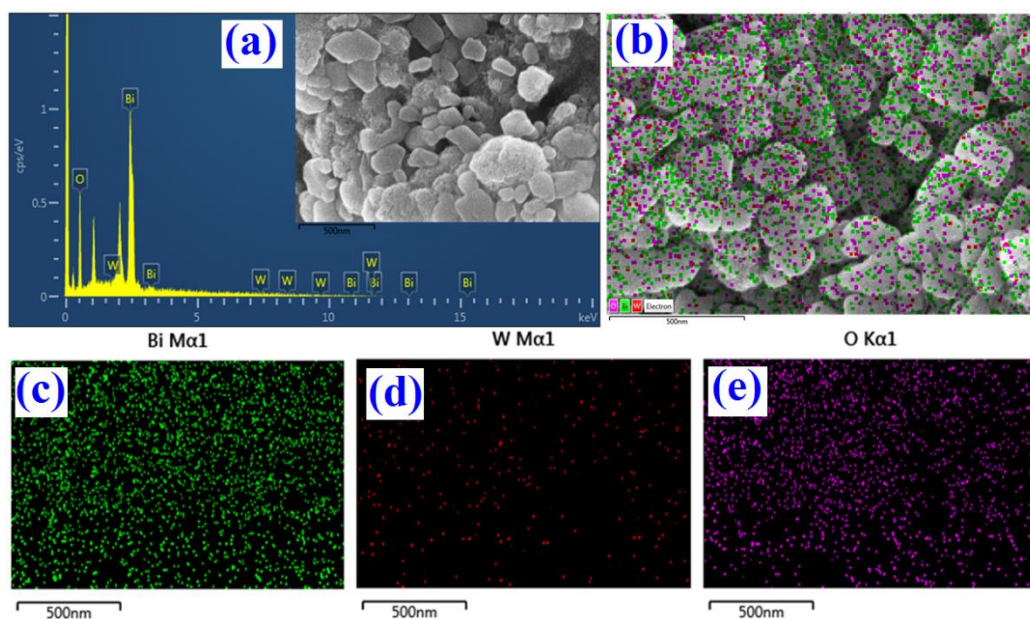


Figure 3. (a) EDX (inset: FE-SEM), (b-e) elemental mapping analysis of Bi_2WO_6 composites.

The morphology of Bi_2WO_6 after calcination process shows the increase in crystalline nature with irregular square nanosheets like structure having the length of 100 nm and was shown in Fig. 2c, d. The EDX spectra (Fig.3a) reveals the chemical composition of samples, which composed of only Bi, W, and O and without any impurity peaks. Fig. 3b-e displays the EDX mapping results; the elements Bi, W, and O are uniformly distributed all over the structure. These results confirm the excellent composition of the Bi_2WO_6 sample.

3.2 Electrochemical behavior of Bi_2WO_6

CV and EIS are very useful techniques for examining the changes in the electrochemical interfacial properties of the different modified electrodes. Fig. 4a shows the Nyquist plot of the bare GCE, WO_6 , and Bi_2WO_6 modified electrodes were fabricated in 0.1 M KCl containing 5 mM $[\text{Fe}(\text{CN})_6]^{3-/4-}$. For bare GCE, the R_{ct} value is 827 Ω at WO_6/GCE the value of R_{ct} was changed to 727 Ω , suggesting that the bare GCE was coated efficiently by WO_6 . A distinct decrease in the R_{ct} was also seen when Bi-modified WO_6 (480 Ω). There is no doubt that Bismuth could improve the conductivity of the tungsten oxide nanoparticles. This result also suggests that $\text{Bi}_2\text{WO}_6/\text{GCE}$ was successfully constructed.

Fig. 4b shows the CV curves of bare, and before and after calcination of Bi_2WO_6 -modified GCE respectively using 0.1 M KCl containing 5 mM of $[\text{Fe}(\text{CN})_6]^{3-/4-}$ at scanning rate 50 mV s^{-1} . $\text{Bi}_2\text{WO}_6/\text{GCE}$ shows higher redox peak current (I_{pa}) separation 62.06 μA compared with bare GCE, and before calcination of Bi_2WO_6 modified electrodes was about 52.7 μA , and 57.0 μA respectively. A smaller R_{ct} value and highest I_{pa} current response were found for the calcined Bi_2WO_6 -modified GCE which depicts the faster electron transfer.

Fig. 4c displays the CV response of Bi_2WO_6 -modified GCE at different scan rates ranges from 20 to 200 mV s^{-1} . Increasing the scan rate when gradually increased redox peaks current. Fig. 4d shows calibration plot between the and redox peak current a square root of scan rate, the result confirms that the modified electrode surface exhibits diffusion-controlled process in general redox reaction of $[\text{Fe}(\text{CN})_6]^{3-/4-}/0.1$ M KCl system. The attained slope value is $I_{pa} (\mu\text{A}) = 6.9929x + 12.234$; $R^2 = 0.9995$, $I_{pc} (\mu\text{A}) = -6.128x - 17.532$; $R^2 = 0.9977$. Furthermore, the Randles-Sevcik equation (1) was used to calculate the surface area of the modified electrodes [28].

$$i_p = 2.69 \times 10^5 A \times D^{1/2} n^{3/2} C v^{1/2} \quad (1)$$

where, A , n , i_p , D , C , and v are represented the electrochemical active area (cm^2), the number of electrons transferred ($1e^-$), anodic peak current, diffusion coefficient, scanning rates (s), and concentration (mol cm^{-3}). The electroactive surface area has been calculated from the obtained slope value. The electroactive area for Bi_2WO_6 -modified GCE was calculated to be 0.36 cm^2 , which is higher than the geometric area of bare GCE before calcination Bi_2WO_6 -modified GCE evaluated as 0.0729 cm^2 , and 0.12 cm^2 , respectively. The result reveals that calcined sample have an improved electrocatalytic active surface area for the electrochemical sensing and has been utilized for the further electrochemical studies,

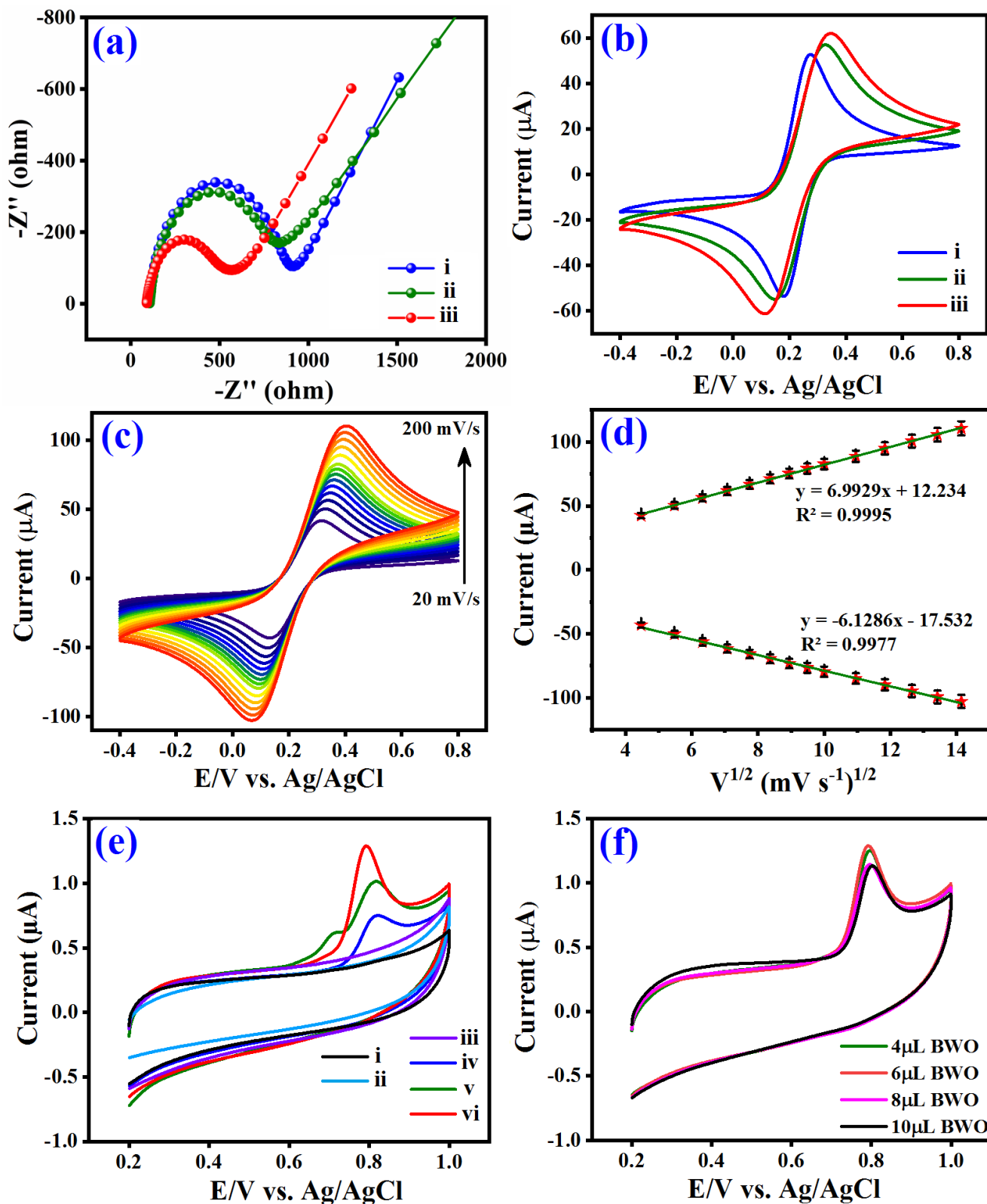


Figure 4. (a) EIS and (b) CV of the (i) bare GCE, (ii, and iii) before and after calcination $\text{Bi}_2\text{WO}_6/\text{GCE}$, (c) different scan rate (20–200 mV s^{-1}) in 0.1 M KCl/5 mM $[\text{Fe}(\text{CN})_6]^{3-/4-}$. (d) linear plot between square root of scan rate and redox peak current, (e) CV of absence and presence 40 μM Sudan I at bare (i, iv) bare GCE, (ii, v) WO_3/GCE and (iii, vi) $\text{Bi}_2\text{WO}_6/\text{GCE}$ and (f) loading capacitance of modified electrodes in 40 μM Sudan I. All experiment conducted in N_2 -saturated PBS (0.05 M, pH 3) at 50 mV s^{-1} .

3.3 Electrochemical performance of Sudan I at Bi₂WO₆/GCE

To study the electrochemical performance of (i, iv) bare GCE, (ii, v) before calcination Bi₂WO₆/GCE, and (iii, vi) after calcination Bi₂WO₆/GCE, CVs were performed absence and presence of Sudan I in PBS (0.05 M, pH 3) at 50 mV s⁻¹ (Fig. 4e). At bare GCE (i), before calcination Bi₂WO₆/GCE (ii), and after calcination Bi₂WO₆/GCE (iii) does not show any obvious electrochemical signal. Then the addition of 40 μM of Sudan I in 0.05 M PBS (pH 3) at bare GCE (iv), before and after calcination Bi₂WO₆/GCE (v, vi). The CV response of GCE was modified with before calcination Bi₂WO₆/GCE showed well defined oxidation peak current at ($I_{pc} = 1.01 \mu\text{A}$) and potential at ($E_{pc} = 0.81 \text{ V}$), Which is demonstrated two proton and two electron transferred oxidation reaction, which is assigned to the oxidation of the -OH group and no reduction peak derived revised scan, indicating irreversible oxidation of Sudan I. The bare GCE shows a very weak anodic peak current ($I_{pa} = 0.75 \mu\text{A}$), and high potential detected for the oxidation of Sudan I at an E_{pa} at 0.82 V. When GCE was modified with before calcination Bi₂WO₆/GCE, the oxidation peak current and potential ($I_{pc} = 1.01 \mu\text{A}$, $E_{pc} = 0.81 \text{ V}$) shifted on the way to the negative side and anodic peak current also increased compared to the bare GCE. A shifting in peak potential ($I_{pc} = 1.3 \mu\text{A}$, $E_{pc} = 0.78 \text{ V}$) and large oxidation peak current and low potential can be detected after calcination of Bi₂WO₆/GCE, owing to its excellent electrochemical activity in the detection of Sudan I

The effect of the loading amount of Bi₂WO₆/GCE (4.0, 6.0, 8.0, and 10.0 μL/1mg mL⁻¹) towards Sudan I sensing was performed by CV in the presence of 40 μM containing PBS (0.05 M, pH 3.0) (Fig. 4f). In Fig. 4f, the highest oxidation current of Sudan I achieved for 6.0 μL (5mg mL⁻¹) compared with other 4.0 μL, 8.0 μL and 10.0 μL Bi₂WO₆ samples. Therefore, 6.0 μL of Bi₂WO₆ modified GCE selected for further electrochemical studies.

3.4 Effect of pH

The electrochemical performance of 40 μM Sudan I at Bi₂WO₆/GCE was further investigated by CV at different pH ranges from 3.0 to 11.0. It can be seen in Fig. 5a that the increases pH value, with the oxidation peak potential, negatively shifted, demonstrating the participating the protons in the electrochemical process. As shown in Fig. 5b, the linear plot between anodic peak potential versus different pH values. The following linear regression equation to be $E_{pa} (\mu\text{A}) = 0.033 (\pm 0.0011) \text{ pH} + 0.8887 (\pm 0.0087)$ ($R^2 = 0.9981$). the obtained slop values from the calibration plot were applied in the Nernst equation to calculated the m/n ratio (eq. 2), [29]

$$E_p = - \left(\frac{0.0592m}{n} \right) \text{pH} + b \quad (2)$$

which m and n are representing the number of protons and electrons. Using equation (2), the calculated m/n ratio is 0.55. The result demonstrated that an equal number of protons and electrons are involved in the reaction. The plausible electrochemical oxidation mechanism was shown in Fig. 5c.

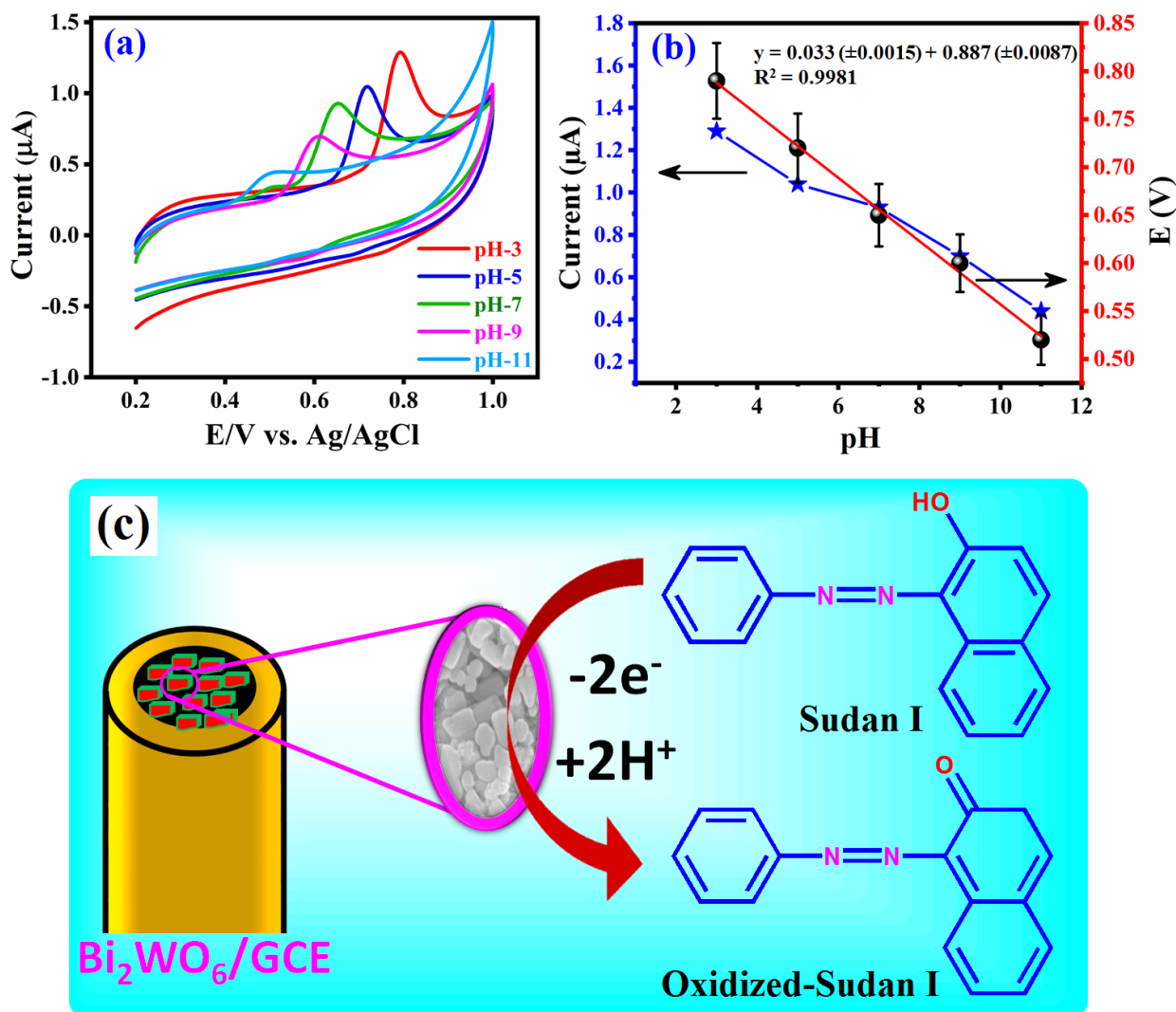


Figure 5. (a) CV response of different pH (3.0–11.0) of 40 μM Sudan I at Bi₂WO₆/GCE at 50 mV s⁻¹, (b) the linear plot of pH versus and peak potential (E_{pa}) and oxidation current and (c) the electrochemical oxidation mechanism.

3.5 Effect of different concentration

Fig. 6a displays the CV response of the various concentrations of Sudan I at Bi₂WO₆ modified GCE in 0.05 M PBS (pH 3) at 50 mV s⁻¹. The increasing concentration of Sudan I from 20 to 120 μM with gradually increased oxidation peaks current response. Fig. 6b displays the linear plot between I_{pc} between the various concentrations of Sudan I, has a good linear relationship ($R^2=0.9934$). The obtained results indicate that the good electrochemical activity and fast electron transfer of Bi₂WO₆/GCE.

3.6 Effect of Scan rate

Fig. 6c showed the CVs of the Bi₂WO₆/GCE electrode in 0.05 M PBS solution in the presence of 20 μM at different scan rates from 20 to 120 mV s⁻¹. The oxidation peak current increased with the increase in scan rate, and the oxidation peak potential shifted to more positively. The oxidation peak

currents were linear with the different scan rates in the ranges from 20–120 mV s^{-1} (Fig. 6d), suggesting an electrode surface exhibits the adsorption controlled process. The linear regression equation is I_p (μA) = 0.0042 (mV s^{-1}) + 0.5143 ($R^2 = 0.9921$). Based on Laviron's equation [30], the electron transfer rate constant (k_s) of the electrochemical sensor was calculated to be 2.78 s^{-1} . The value of k_s is higher than those of other modified electrodes. For irreversible electrode reaction, the number of an electron (n), can be obtained from the equation,

$$\alpha n = \frac{47.7}{E_p - E_{p/2}} \quad (3)$$

E_p and $E_{p/2}$ are represented by peak potential and formal potential at with ($I = I_{p/2}$ in CV), α is the electron transfer coefficient, respectively. In this work $E_p = 0.79$, and $E_{p/2} = 0.75 \text{ V}$. therefore, αn was calculated to be 1.19. Generally, α is assumed to be 0.5 (irreversible electrode process). So two electrons are involved in the electrochemical reaction.

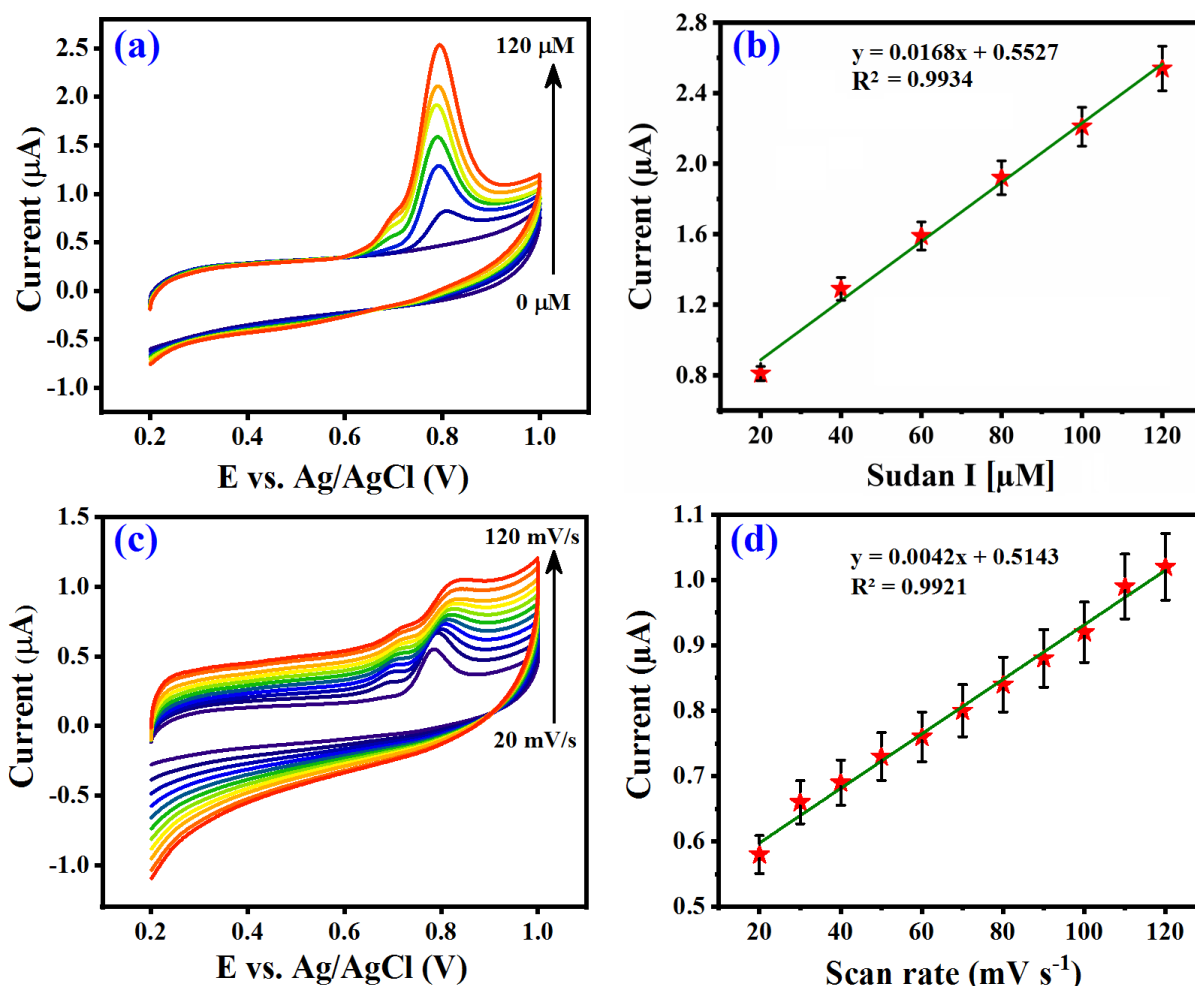


Figure 6. (a) CVs of Bi₂WO₆/GCE in different concentration of Sudan I (20–120 μM) in PBS (0.05M, pH 3), at 50 mV s^{-1} , (b) The linear plot for I_{pc} and different concentration of Sudan I. (c) CVs of 20 μM Sudan I in PBS (0.05M, pH 3) at different scan rates (20–120 mV s^{-1} at Bi₂WO₆/GCE. (d) Plot amongst the scan rate versus anodic peak current.

3.7 Determination of Sudan I

Fig. 7a shows the DPV analysis of Sudan I at the Bi₂WO₆ modified electrodes. The anodic peak current increased with increase in concentration of Sudan I within the range from 0.02 to 114.6 μM. As shown in Fig. 7b, the plot between anodic peak current proportional to its Sudan I concentration, which is two linear range were obtained in the ranges of 0.02–9.00, and 40–114.6 μM. the first regression equation is $I_p = 0.1114 [\mu\text{M}] + 0.309$ ($R^2 = 0.9911$) and $I_p = 0.0272 [\mu\text{M}] + 0.7692$ ($R^2 = 0.9795$). Fig. 7b inset shows anodic peak current at lower concentration level. The detection limit at Bi₂WO₆/GCE was estimated to be 0.005 μM (S/N=3) and sensitivity is 3.0563 μA μM⁻¹, which is comparable to those of some other reported electrodes shown in Table 1. The fabricated Bi₂WO₆/GCE sensor has been used as a promising electrode material for the highly efficient electrochemical detection for Sudan I.

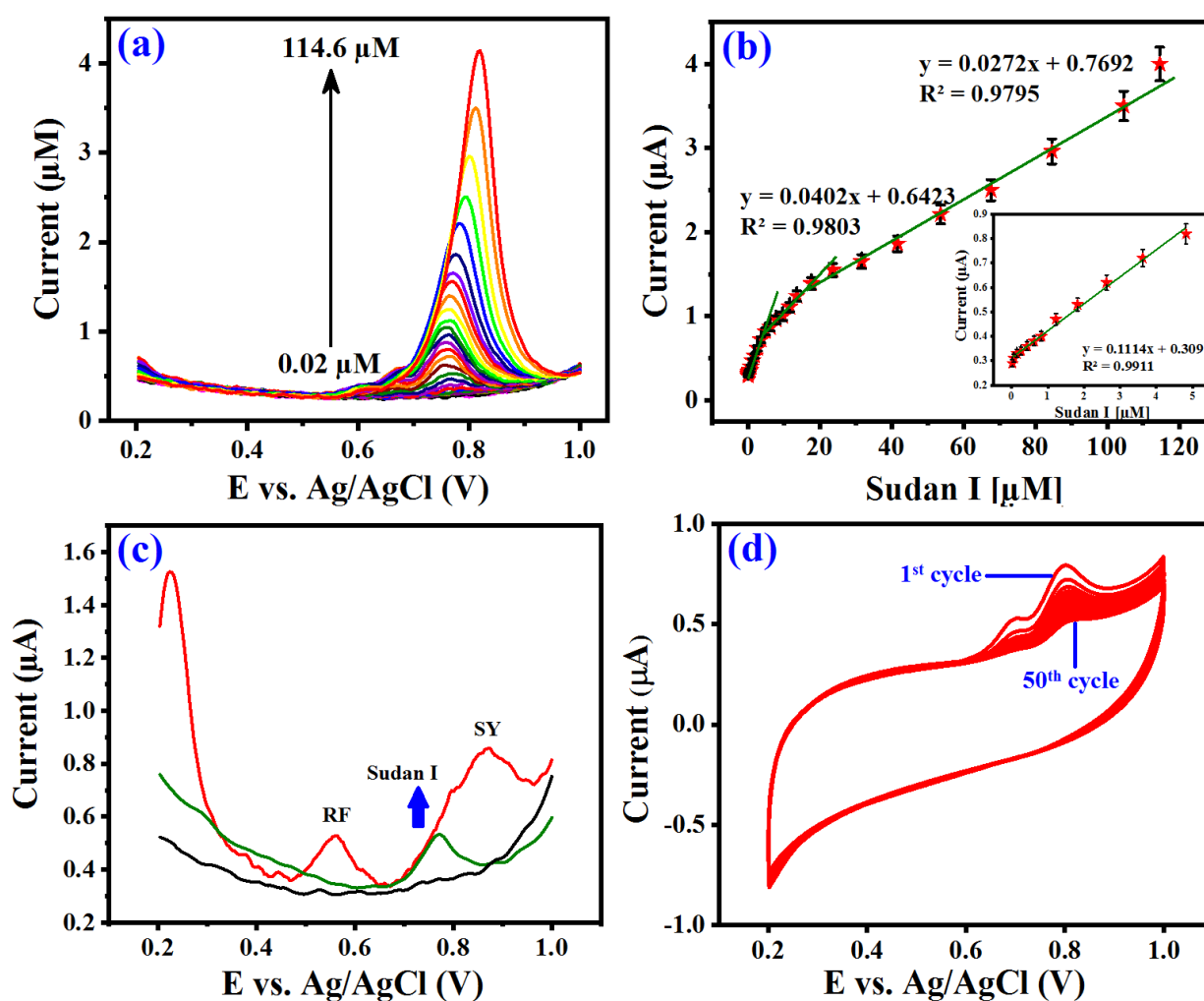


Figure 7. (a) DPV curves of Bi₂WO₆-modified GCE with various concentration Sudan I from 0.02 to 114.6 μM in 0.05 M PBS (pH 3). (b) Linear calibration plot between concentrations of Sudan I vs. oxidation peak current, (c) simultaneous determination DPV response of RF, SY, and Sudan I electroactive molecules, and (d) stability of 50 cycles in the presence of 20 μM of Sudan I.

Table 1. The determination of Sudan I with different electrodes Bi₂WO₆-modified GCE

Electrode	Linear range (μM)	LOD (μM)	Ref.
poly(p-ABSA) ^a /GCE	1 – 500	0.3	31
AgNPs@GO ^b /GCE	3.90 – 31.9	1.14	32
AuNPs/RGO/GCE	0.01 – 70	0.001	33
NiFe ₂ O ₄ /SPE ^c	0 – 100	0.05	34
Graphene/ β -CD ^d /PtNPs ^e /GCE	0.005 – 68.68	1.6 nM	35
La ³⁺ -Co ₃ O ₄ /SPE	0.3 – 300	0.05	36
Au ^f /MIP ^g	0.01 – 10	0.002	37
Ag-Cu/rGO/GCE	0.001 – 10	0.4 nm	38
PIL ^h -EG ⁱ /GCE	0.0686 – 8.79	0.023	39
CuO-ITO ^j	0.001 – 1.56	120	40
PVP ^k /ZnSe-CTAB ^l -GR/GCE	0.004 – 15.0	0.5	41
CuO/3DNPC ⁿ /GCE	2.5 – 100	0.84	42
Bi ₂ WO ₆ /GCE	0.02 – 114.6	0.005	This work

^apoly (p-aminobenzene sulphonic acid), ^bgraphene oxide, ^cscreen printed electrode, ^d β -cyclodextrin, ^eplatinum nanoparticles, ^fgold, ^gmolecular imprinted, ^hpoly (ionic liquid), ⁱelectrochemical reduced graphene, ^jindium tin oxide, ^kpolyvinylpyrrolidone, ^lcetyl trimethylammonium bromide, ⁿ3D N-doped porous carbon

3.8 Interference, reusability, and reproducibility

Anti-interference ability is an important factor for the electrochemical sensor. Fig. 7c displayed the simultaneous DPV responses towards rifampicin (RF), sunset yellow (SY), and Sudan I electroactive molecules. Moreover, the DPV response shows a specified potential for Sudan I than that of other interferents. The other interference of some organic compound coexisting the DPV response of Sudan I was acquired is and highly selective determination and anions and cations studied. The organic compounds such as the 50-fold concentration of ascorbic acid, glucose, citric acid, glutamic acid, and the 50-fold concentration of anions and cations such as Na⁺, Ca²⁺, Zn²⁺, Cl⁻, CO₃²⁻, and SO₄²⁻ (figure not shown).

The stability of the developed sensor was studied to the stability test for 50 cycles in pH 3.0 (0.05 M PBS) 20 μM Sudan I. The CV studies at Bi₂WO₆/GCE exhibited the highly stable response for 50 cycles with the current retention of 84% from the initial value (Fig. 8a). The long-term stability of the fabricated sensor was examined by determining the anodic current of 20 μM Sudan I. The developed sensor maintains about 94.5% of its initial anodic peak current response after 12 days, which suggests that the Bi₂WO₆-modified electrode has the high storage stability.

The reproducibility of the developed sensor was also studied and was shown in (Fig. 8b). The reproducibility of the fabricated sensor was examined by the anodic peak current response of 20 μM Sudan I in pH 3.0 (0.05 M PBS) using five different modified electrodes, they were developed by under

optimum condition. The obtained current response changes, the relative standard deviation (RSD %) of five different modified electrodes is about 2.86%, which demonstrates that the fabricated sensor has good reproducibility.

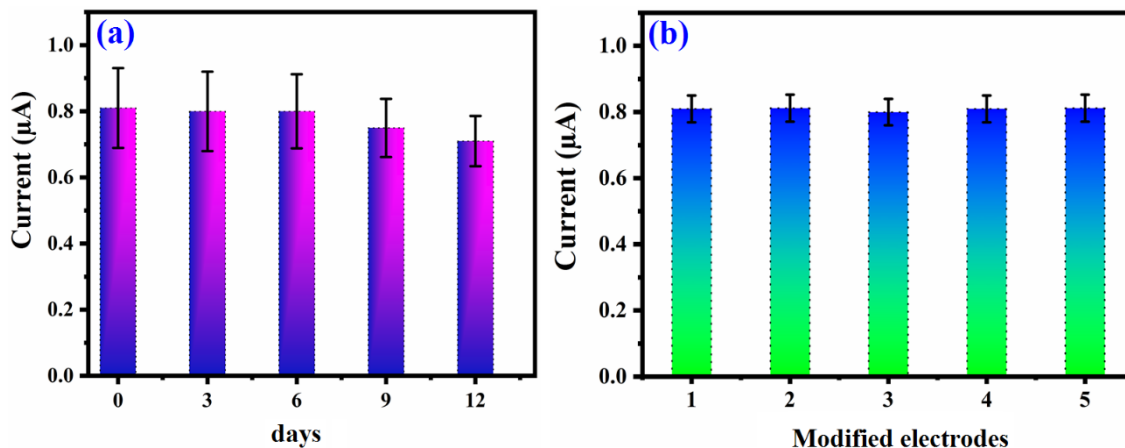


Figure 8. CV response of (a) storage stability of modified electrode for electro-oxidation of Sudan I response after being kept for 12 days, (b) reproducibility of modified electrodes. All measurements recorded in N₂-saturated 0.05 PBS with 20 μM Sudan I at 50 mV s⁻¹.

3.9 Real sample analysis

Table 2. Detection of Sudan I in water samples using Bi₂WO₆-modified GCE

Sample	Concentration of Sudan I		*Recovery % (mean± RSD) (n=3)
	Spiked (μM)	Found (μM)	
Apple juice	1.5	98.2	98.2 ± 0.024
	2.0	98.6	98.6 ± 0.013
	2.5	97.2	97.2 ± 0.028
	3.0	98	98 ± 0.042
	3.5	99	99.1 ± 0.041
Chili powder	1.0	96.8	96.8 ± 0.026
	1.7	97.9	97.9 ± 0.068
	2.0	97.5	97.5 ± 0.053
	2.5	98.4	98.4 ± 0.058

* Relative Standard Deviation of three individual measurements.

To evaluate the practicability of Bi₂WO₆-modified electrodes based detection of Sudan I, real-time analysis was carried out in apple juice and chili powder samples. Both samples were collected from

the local market, Taiwan. The real samples spiked in foodstuffs such as apple juice and chili powder samples by the spiked method was conducted for the recovery of Sudan I in real samples. DPV was used to estimate the determination of Sudan I from the real samples at pH 3 (0.05 PBS) as shown in Fig. 9. The anodic peak current response of the samples was measured and Table 2 displayed the observed recovery results. The satisfactory recovery results are attained in apple juice (97.2 to 99.1%), and chili powder samples (96.8 to 98.4%), respectively. The acceptable recoveries of all the real samples confirm the developed sensor has high accuracy and reliability for the determination of Sudan I in real samples.

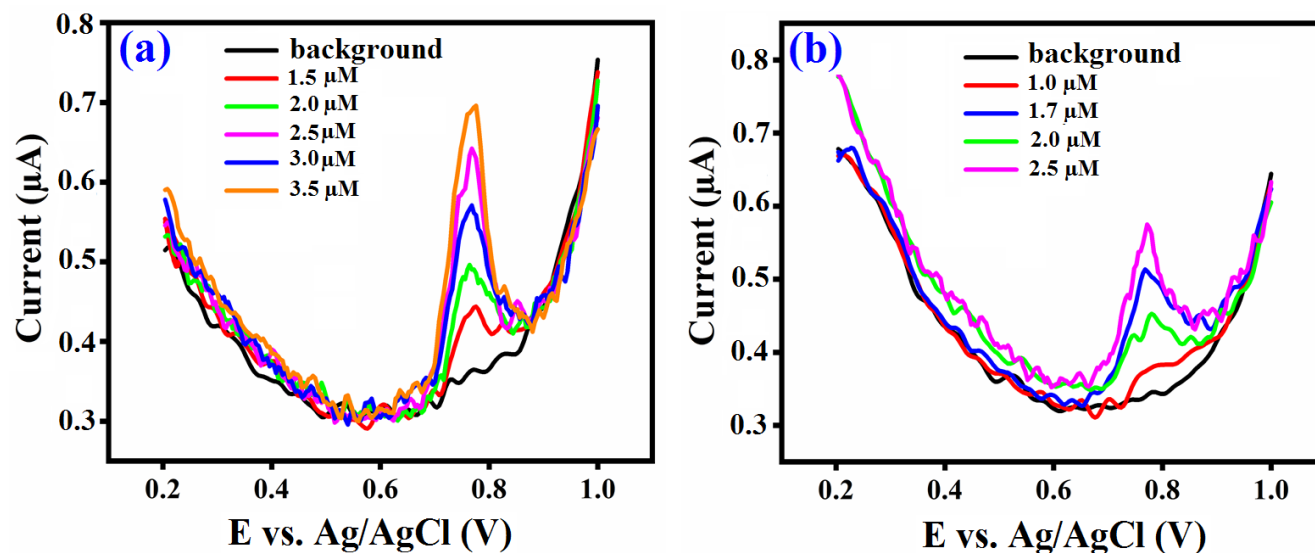


Figure 9. (a and b) Real samples analysis of DPV response of Bi₂WO₆-modified GCE with various concentrations spiked Sudan I.

4. CONCLUSION

In conclusion, Bi₂WO₆ was synthesized by the co-precipitation method and used for the electrochemical determination of Sudan I dye. Bi₂WO₆ nanosheets were obtained after calcination and characterized by XRD, FE-SEM-with EDX, and EDX-elements mapping analysis. We developed an electrochemical sensor for the determination of Sudan I using Bi₂WO₆/GCE. The electrochemical properties of the Bi₂WO₆ modified electrodes were investigated thoroughly. Hence, this work demonstrated a very low detection limit of 0.005 μM (S/N=3) with good sensitivity is 3.0563 μA μM⁻¹. Besides, the fabricated sensor achieved good stability, excellent reproducibility also selectivity for the detection of Sudan I. The as-prepared Bi₂WO₆/GCE sensor successfully applied to sensing Sudan I in different real samples with acceptable recoveries. In addition, Bi₂WO₆/GCE sensor showing better electrochemical behavior and can be apply to the future modern sensing devices.

ACKNOWLEDGEMENTS

The authors are grateful for the financial support (MOST 107-2113-M-027-005-MY3 to S.M.C) from the Ministry of Science and Technology (MOST), Taiwan.

ORCID

Arumugam Sangili: 0000-0001-9628-0067

Shen-Ming Chen: 0000-0002-8605-643X

References

1. J. Li, H. Feng, J. Li, Y. Feng, Y. Zhang, J. Jiang and D. Qian, *Electrochim. Acta*, 167 (2015) 226-36.
2. D. M. Marmion, Handbook of US colorants for food, drugs, and cosmetics (No. 614.3 M3) 1979.
3. M. Stiborová, V. Martínek, H. Rýdlová, P. Hodek and E. Frei, *Cancer Res.*, 62 (2002) 5678.
4. H. Yan, H. Wang, J. Qiao and G. Yang, *J. Chromatogr.*, 1218 (2011) 2182.
5. L. He, Y. Su, X. Shen, Z. Zeng and Y. Liu, *Anal. Chim. Acta*, 594 (2007) 139.
6. E. Ertaş, H. Özer and C. Alasalvar, *Food Chem.*, 105 (2007) 756.
7. F. Tateo and M. Bononi, *Food Chem.*, 52 (2004) 655.
8. M. I. López, I. Ruisánchez and M. P. Callao, *Spectrochim. Acta A*, 111 (2013) 237.
9. M. Ávila, M. Zougagh, A. Escarpa and Á. Ríos, *J. Supercrit. Fluid.*, 55 (2011) 977.
10. J. Zhang, M. L. Wang, C. Shentu, W. C. Wang, Y. He and Z. D. Chen, *J. Electroanal. Chem.*, 685 (2012) 47.
11. J. Yu and A. Kudo, *Adv. Funct. Mater.*, 16 (2006) 2163.
12. Y. Liu, Z. H. Yang, P. P. Song, R. Xu and H. Wang, *Appl. Surf. Sci.*, 423 (2018) 561.
13. A. Umar, R. Ahmad, R. Kumar, A. A. Ibrahim and S. Baskoutas, *J. Alloys Comp.*, 683 (2016) 433.
14. W. Mao, B. Cai, Z. Ye and J. Huang, *Sens. Actuators B Chem.*, 261 (2018) 385.
15. L. Peng, S. Dong, H. Xie, G. Gu, Z. He, J. Lu and T. Huang, *J. Electroanal. Chem.*, 726 (2014) 15.
16. S. H. Yu, B. Liu, M. S. Mo, J. H. Huang, X. M. Liu and Y. T. Qian, *Adv. Funct. Mater.* 13 (2003) 639.
17. D. Wang, Y. Zhen, G. Xue, F. Fu, X. Liu, D. Li, *J. Mater. Chem. C*, 1 (2013) 4153.
18. C. Li, G. Chen, J. Sun, Y. Feng, J. Liu and H. Dong, *Appl. Catal. B Environ.*, 163 (2015) 415.
19. K. Li, P. Zheng, L. Tong, D. Ren, M. Xu, X. Tang and X. Liu, *Compos. Part B-Eng.* 176 (2019) 107202.
20. W. Qu, W. Wlodarski and J. U. Meyer, *Sens. Actuators B Chem.*, 64 (2000) 76.
21. Z. Lou, J. Deng, L. Wang, L. Wang and T. Zhang, *Sens. Actuators B Chem.*, 82 (2013) 217.
22. U. Rajaji, M. Govindasamy, S. M. Chen, T. W. Chen, X. Liu, and S. Chinnapaiyan, *Compos. Part B Eng.*, 152 (2018) 220.
23. A. Muthumariyappan, U. Rajaji, S. M. Chen, T. W. Chen, Y. L. Li and R. J. Ramalingam, *Ultrason. sonochem.*, 57 (2019) 233.
24. H. M. Moghaddam, S. Tajik and H. Beitollahi, *Food chem.*, 286 (2019) 191.
25. Y. Qin, H. Li, J. Lu, Y. Ding, C. Ma, X. Liu, Z. Liu, P. Huo and Y. Yan, *Appl. Surf. Sci.*, 48 (2019) 1313.
26. T. Nagyné-Kovács, G. Shahnazarova, I. E. Lukács, A. Szabó, K. Hernadi, T. Igricz, K. László, I. M. Szilágyi and G. Pokol, *Materials*, 12 (2019) 1728.
27. A. Kaur and S. K Kansal, *Chem. Eng. J.*, 302 (2016) 194.
28. G. Leftheriotis, S. Papaefthimiou, P. Yianoulis, *Solid State Ion.* 173 (2007) 259-63.
29. A. Sangili, M. Annalakshmi, S. M. Chen, P. Balasubramanian, M. Sundrarajan, *Compos. Part B-Eng.* 162 (2019) 33-42.
30. H. Yin, Y. Zhou, X. Meng, T. Tang, S. Ai and L. Zhu, *Food chem.*, 127 (2011) 1348.

31. B. L. Li, J. H. Luo, H. Q. Luo, N. B. Li, *Food chem.*, 173 (2015) 594.
32. E. Prabakaran and K. Pandian, *Food chem.*, 166 (2015) 198-205.
33. J. Li, H. Feng, J. Li, Y. Feng, Y. Zhang, J. Jiang and D. Qian, *Electrochim. Acta*, 167 (2015) 226.
34. H. Beitollahi, S. Tajik, S. Jahani and N. F. Gargani, *Anal. Bioanal. Electrochem.*, 10 (2018) 1317.
35. S. Palanisamy, T. Kokulnathan, S. M. Chen, V. Velusamy, S. K. Ramaraj, *J. Electroanal. Chem.*, 794 (2017) 64.
36. H. M. Moghaddam, S. Tajik and H. Beitollahi, *Food chem.*, 286 (2019) 191.
37. S. Chen, D. Du, J. Huang, A. Zhang, H. Tu, A. Zhang, *Talanta*, 84 (2011) 451.
38. Y. Yao, Y. Liu and Z. Yang, *Microchim. Acta*, 183 (2016) 3275.
39. L. Li, X. Liu, J. Lu, Y. Liu and X. Lu, *Anal. Methods*, 7 (2015) 6595.
40. M. M. Tunesi, N. H. Kalwar, R. A. Soomro, S. Karakus, S. Jawaid and M. I. Abro, *Mat. Sci. Semicon. Proc.*, 75 (2018) 296.
41. K. Karaboduk and E. Hasdemir, *Food technol. Biotech.*, 56 (2018) 573.
42. Q. Ye, X. Chen, J. Yang, D. Wu, J. Ma and Y. Kong, *Food chem.*, 287 (2019) 375.

© 2020 The Authors. Published by ESG (www.electrochemsci.org). This article is an open access article distributed under the terms and conditions of the Creative Commons Attribution license (<http://creativecommons.org/licenses/by/4.0/>).